

# SPECTROSCOPIC STUDY OF A CUTTING ELECTRICAL ARC IN H.B.C FUSE

W.Bussière, P. Bezborodko, R. Pellet  
William.BUSSIERE@laept.univ-bpclermont.fr  
pierre.bezborodko@laept.univ-bpclermont.fr  
Rene.PELLETT@laept.univ-bpclermont.fr

Laboratoire Arc Electrique et Plasmas Thermiques (LAEPT) - Université Blaise-Pascal  
CNRS UPES-A 6069 - 24, Avenue des Landais - F 63177 AUBIERE Cedex - France

**Abstract:** This paper describes an experimental set up used to investigate the physic parameters of the arc, in fact the temperature and the electron density. Improvements have been made from the last set up [1]. Fuses studied here are High Breaking Capacity fuses (HBC). In this study, the arc dissipates 1,200 J, the peak of current is about 2,000 A and the duration of the arc is 3 ms. The whole of the visible spectrum has been registered, from 360 nm to 800 nm, in the exploding part of the arc. The spectrum consists of continuous light together with spectral lines which appears mostly when the electric current decreases. The behaviour of the spectra shows that there is a big gradient of species concentrations in the arc, together with a high gradient of temperature.

The temperature is measured from Si II lines and metallic spectral transitions. The calculations show a decrease from about 17,000 K at the beginning of the phenomenon, until about 7,000 K at 4 ms after the beginning of the electric current. The measured values of the electron density vary between  $10^{17}\text{cm}^{-3}$  and  $10^{19}\text{cm}^{-3}$ .

## I. INTRODUCTION

We briefly recall the specifications of the experimental fuse we use. We know that there exist very close interactions between the arc and the surrounding sand : so it is necessary to keep, as far as possible, the similar properties of the arc and its sand coating as in an industrial fuse. In an industrial fuse, it is not possible to collect suitable light because of the scattering of light by the sand grains. To completely avoid the scattering of light, one side of the experimental fuse consists of a 4-mm wide glass wall ; the fuse element in silver or in copper is directly put on it. On the other side, the fuse is filled with silica grains with a mean diameter of 0.4 mm. We distinguish two different experimental fuses, depending on the position of the fuse element on the glass wall (Figure I). In the experimental fuse (b) (in opposition to the experimental fuse (a)), the section of the fuse element is directly put on the glass wall : the area of the fuse element in contact with the glass wall is thus less important, and interactions between this two elements are weaker. Fulgurites obtained with the

experimental fuses (a) do not have the same shape as industrial ones, whereas those obtained with the experimental fuses (b) are nearly identical.

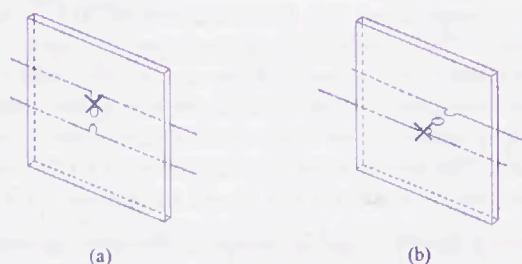


Figure I - Experimental fuses (a) and (b); the cross symbolizes the observation point.

It has been verified previously that the compactness of sand is an essential factor to obtain a good electrical cut off. In the same way, the spectra obtained later closely depend on the apparent density of sand, which is the reason why the mass of sand is checked for each fuse box.

Our fuse elements have an effective length of 36 mm, are 0.105 mm thick, 5 mm wide, and are 99.99 % pure silver (or copper). They have a single row of notches (0.5 mm in diameter) punched in the centre of the strip.

## II. EXPERIMENTAL SET UP: SPECTROSCOPIC ACQUISITIONS USING KINETIC MODE

### II.1 Light collection

The light coming from the glass wall is accurately collected via an optic fibre connected to the input of a spectroscope. The exact location of viewing is determined by way of a small laser beam. The

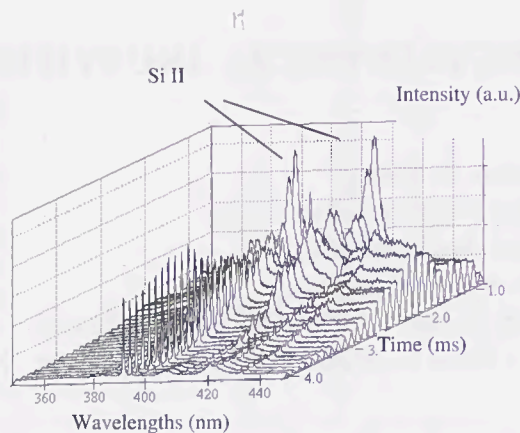


Figure II - Visible spectra obtained within [360-440] nm. The pre-arcing value is 0.87 ms.

spectroscope used is a Chromex 500 IS (0.5-m focal length). Three diffraction gratings can be used: 600; 1,200 and 1,800-gr/mm. As the aim of this work is to obtain the global visible spectra, the 600-gr/mm grating has been used in most cases. So, the bandwidth is about 90 nm. The output light is collected by a CCD matrix whose size is  $1,242 \times 1,152$  pixels. Each pixel is a  $22.5\text{-}\mu\text{m}$  side square. The 1,800-gr/mm diffraction grating is used for the evaluation of the electron density : it provides a 25-nm bandwidth.

## II.2 Use of matrix in a kinetic mode

The matrix is 1,152 lines high. It is divided in 39 tracks, 29 lines each. An area of 21 lines, on the bottom of the matrix, is never used. The spot light is aimed on the first track located at the bottom (pixels 1,131 to 1,102). Shortly before the phenomenon the mechanical shutter is open. At the beginning ( $t = 0$  ms), one imposes to the matrix  $15\ \mu\text{s}$  of time exposure. Then the shifting up of the content of lines is commanded, line after line, and this, 29 times. Shifting of one line requiring  $3\ \mu\text{s}$ , then,  $87\ \mu\text{s}$  after, the totality of the track is in the upper track (1,102-1,073). Now,  $t = 87 + 15 = 102\ \mu\text{s}$ . A time exposure of  $15\ \mu\text{s}$  is imposed again and so on until the totality of the matrix is full, at  $t = 39 \times 102\ \mu\text{s} = 3.98$  ms. The mechanical shutter is then closed, with a non reproducible long time lag.

The first and the last tracks are randomly exposed because of the inaccuracy of the mechanical shutter. For this reason these spectra are not shown later in this paper.

An electronic circuit drives simultaneously the start of the power supply and the shifting of the matrix. For each shooting, the start of the power supply, the current flowing across the fuse and the voltage drop are stored by means of two oscilloscopes.

## III. EXPERIMENTAL RESULTS AND DISCUSSION

### III.1 Evolution of radiation versus time

The whole of the visible spectrum has been registered from 360 to 800 nm [2]; each spectrum has an approximate 90-nm bandwidth, the total spectrum is a juxtaposition of 6 spectra. To avoid possible problems of reproductibility, three discharges are done for each wavelength.

Figure II reveals a typical evolution of spectra obtained for a single discharge.

We easily distinguish three different stages in the global spectrum :

- Spectral transitions which are superimposed on an intense continuous light : it corresponds to the meantime 0.8 to 1.4 ms after the beginning of the current.
- Increase of the continuous light which dominates the whole spectrum from 1.4 to 2.5 ms. Continuous light is most important in the I.R. than in the U.V. region because of the increase of the free-free transitions. Some atomic transitions are still emitted : the latters correspond to ionised species.
- The continuous light decreases fastly and atomic transitions emerge from 2.5 ms until the end of the phenomenon.

This evolution is observed in the two models of experimental fuses.

To determine the temperatures from spectral lines, we need to know precisely the origin of light. In particular we need to know whether there is a continuous light at the foot of lines or whether some specific lines are sufficiently isolated in the spectrum. For these reasons our first measurements are devoted to identify all the species which emit light in arc fuses. The totality of the visible spectrum was first studied within 3 ms after the beginning of the arc, because the narrowness of lines permits a very good estimation of wavelengths. An accurate gauging of the spectrometer had been realised with spectral lamps, it had showed that the wavelength of a line was given with an absolute accuracy of 0.07 nm.

The recognition of emitting species has required several sources. Several spectral tables have been used [3][4][5], as well as data referring to N.I.S.T. [6]. Nevertheless, this information is often insufficient because for a given wavelength there are a lot of corresponding elements. So, one has to study each atomic transition in detail.

Three groups of spectral lines have been identified (Table I) :

- The impurities : they are present in the sand and especially in the glass wall ; they consist of oxide such as CaO, Na<sub>2</sub>O, K<sub>2</sub>O. All the impurity species singled out emit resonance lines (atomic transitions to the ground state).
- The metallic transitions (Ag and Cu) : we only observed neutral atomic transitions.
- The silicon transitions : observed in the neutral state and ionised once.

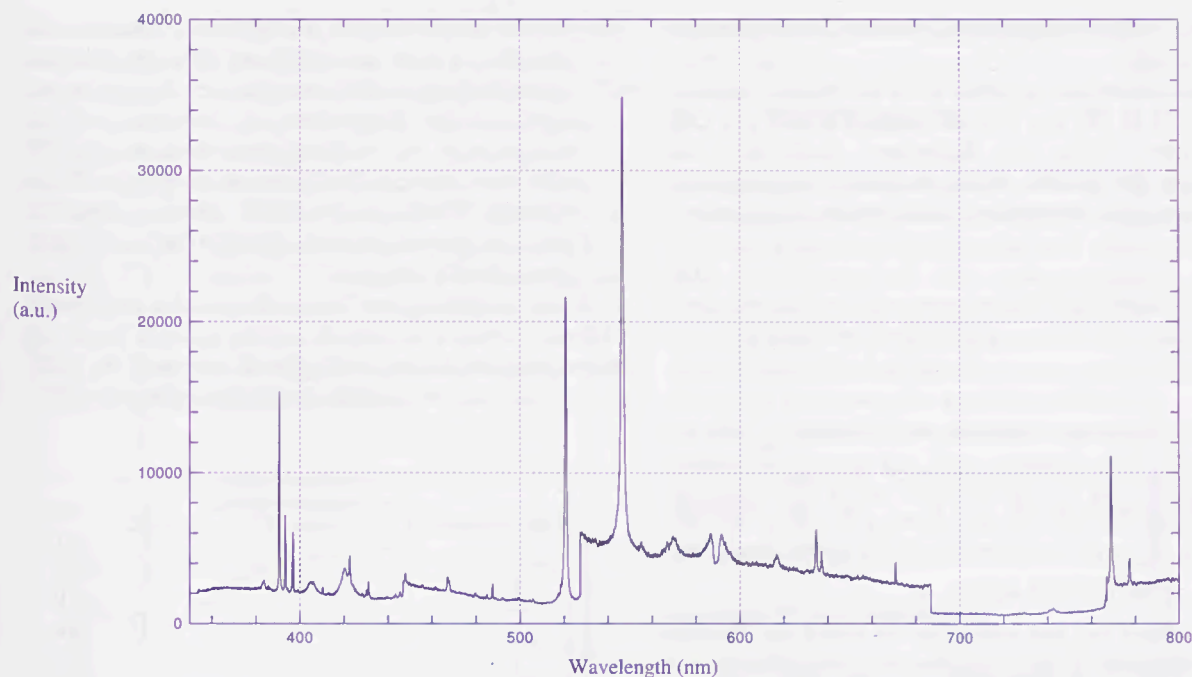


Figure III – Visible spectrum obtained 3.0 ms after the beginning of the arc.

Element	Ionization stage	$\lambda_{\text{THEORETICAL}}$ (nm)
Si	II	385.60
Si	II	386.26
Si	I	390.55
Ca (R)	II	393.37
Ca (R)	II	396.85
Si	II	412.81
Ca (R)	I	422.67
Ag	I	431.11
Ag	I	447.61
Ag	I	466.85
Ag	I	487.42
Ag (R)	I	520.91
Ag (R)	I	546.55
Na (R)	I	588.99
Na (R)	I	589.59
Si	II	634.71
Si	II	637.14
Li (R)	I	670.78
Li (R)	I	670.79
K (R)	I	766.49
K (R)	I	769.90
Ag	I	768.78
O	I	777.19
O	I	777.42
O	I	777.54

Table I – Identified transitions in fuse tests within the spectral band [360-800] nanometers. Tests done with copper fuse element revealed the  $\lambda = 510, 515, 521$  nm lines.

Within 3 ms, twenty five lines are identified with certainty (Figure III).

### III.2 Plasma temperature evaluation using the ionised silicon multiplets (1) and (3)

Among the atomic transitions identified, we have used the groups of the metallic transitions and the silicon transitions ionised once to evaluate the temperature.

As first approximation, we compare the arc in a fuse with a wall stabilised arc, the arc being closed within molten silica. In such case, it is known that metallic particules spread to the walls and the electrodes. As a consequence, we can expect to obtain different temperature values from the two groups of atomic transitions. In fact, to make calculation from lines, we have to use lines from elements which are first present in the centre of the arc and second which emitted some light at high temperature because at the beginning of

the arc's growth, temperatures in the arc are supposed to be very high.

Calculations are achieved from the relative intensity ratio of Si II 386 nm (2D-2P°) and Si II 413 nm (2D-2F°) lines. Using the Boltzmann distribution and assuming the plasma being in local thermodynamic equilibrium, the temperature at the instant  $t$  is given by :

$$T(t) = \frac{E_{m1} - E_{m2}}{k} \times \frac{1}{\log \left( \frac{g_{m1} A_{mn1} \lambda_{mn2} J(\lambda_{mn2}, t)}{g_{m2} A_{mn2} \lambda_{mn1} J(\lambda_{mn1}, t)} \right)} \quad (1)$$

where  $A_{mn1,2}$  are the transition probabilities,  $\lambda_{mn1,2}$  are the differences in wavelength between the upper levels  $m$  and the deeper levels  $n$ ,  $g_{m1,2}$  are the statistical weights,  $E_{m1,2}$  are the energies of the upper levels, and  $J(\lambda_{mn1,2}, t)$  are the lines areas.

This method has the advantage to avoid an absolute light calibration of the experimental set up. Moreover, it is not necessary to know the species concentrations. The experimental uncertainties come from spectroscopic data (especially the transition probabilities) and from the difficulty to estimate the line area, which overlaps a not-to-well defined shape of continuum. As the influence of pressure on radiation is not well known, we decided to use maximal intensities, rather than lines areas.

Calculations (Figure IV) have been made using spectra obtained from the two models of the experimental fuse.

We can summarize the results in three points :

- We observe a logical decrease of temperature in the meantime 0.9-3.0 ms ; fuse is in fact a device used to dissipate energy.
- In spite of this logical evolution, we notice a weak variation during the studied meantime. Values are still high at the end of the phenomenon.
- The discrepancies between the two types of results are justified as follows : in the case of the experimental fuse (a), the fuse element is directly put on the glass wall ; it involves the shifting of the plasma on the glass wall. On the contrary, in the case of the experimental fuse (b), the energy is closely concentrated in an ionised channel whose expansion is limited by the surrounding compact silica sand ; fulgurites obtained have a shape as good as in industrial fuses.

Evaluations have also been made using the Cu I  $\lambda = 510, 515$  and  $521$  nm lines at the end of the phenomenon in the case of the experimental fuse (b). We were motivated by two goals :

- We wanted to evaluate discrepancies between the temperature obtained from the maximal intensities ratio of ionised silicon lines and from metallic transitions.

- As the profil shapes are easier to observe, we compared values deduced from (1) using maximal intensities ratios and areas ratios. As continuous light is less important at the end of the phenomenon, we worked in the meantime 3.0-4.0 ms : from the maximal intensities we got values between 7,500K and 6,000K, whereas from the areas we got values between 12,500K and 9,500K (gaussian line shapes).

Thus we notice that the scales of size are clearly different between the silicon and the metallic lines, and that numerical values are higher if one uses the areas ratio rather than the maximal intensities ratio.

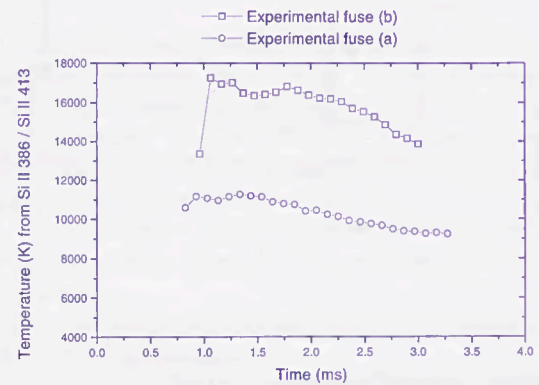


Figure IV - Temperatures obtained from the Si II  $\lambda = 386$  nm and 413 nm lines. Results are given for the two models of experimental fuses.

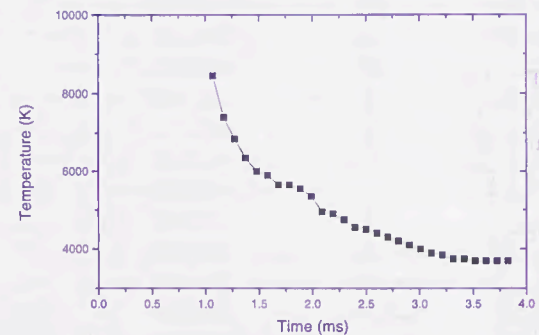


Figure V - Low threshold temperature deduced from the Planck's law within [360-800] nm for the experimental fuse (a).

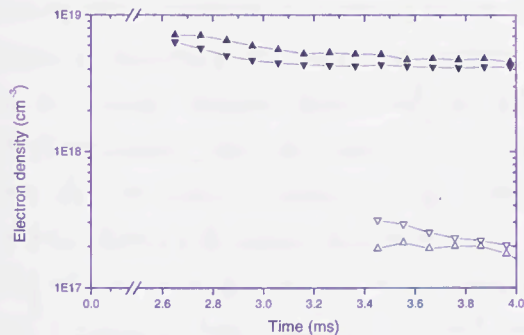
### III.3 Black body approximation

In order to improve our knowledge of the physical parameters of the plasma, we tried to characterize the plasma radiation during the meantime 1.4-2.5 ms. As there is no spectral line observed in some spectral intervals such as in [670-760] nm, we tried to evaluate the temperature by making the comparison between a

black body curve at given temperature and our spectra, within [360-800] nm. We have used the Planck's law assuming an emission coefficient equal to unity. This implies to obtain a low threshold of the temperature. Results are shown in Figure V.

The temperature obtained decreases roughly from 8,000K to 3,000K. This evolution is still logical, but the values are not available because one ignores the layer on which the radiation is integrated ; and an emission coefficient below unity should involve higher values.

#### III.4 Electron density deduced from the ionised silicon multiplet (2) Stark shifts



Fi

Figure VI - Electron densities for the two models of experimental fuses for  $T = 15,000$  K : -▼- Si II  $\lambda = 634$  nm, experimental fuse (b) ; -▲- Si II  $\lambda = 637$  nm, experimental fuse (b) ; -▽- Si II  $\lambda = 634$  nm, experimental fuse (a) ; -△- Si II  $\lambda = 637$  nm, experimental fuse (a).

To obtain an evaluation of the electron density, we did not use the line shape and thus the broadening parameters because of the difficulties we had for fitting line shapes. Thus we deduced the electron density from the shift between theoretical and experimental wavelengths.

This method is applied to the ionised silicon multiplet (2). We suppose that the observed shifts of the  $\lambda = 634.7$  and  $637.1$  nm lines are due to the Stark effect. From the theoretical values of shifts given by Griem [7] as a function of temperature and at a given density, and according to the fact that Stark effect is a linear function of the electron density and a non linear function of the temperature, we deduce the values of the electron density versus time by observing the experimental shifts. Because of the weak change of the shifts with the temperature, calculations are carried out with a temperature equal to 15,000 K.

Results are given in the Figure VI for the two models of experimental fuses. The results obtained with the experimental fuse (b) are rather in good agreement with Chikata's one [8] : between  $4 \times 10^{18} \text{cm}^{-3}$  and  $8 \times 10^{18} \text{cm}^{-3}$  ; whereas the results issued from the

experimental fuse (a) are rather in the range  $2-4 \times 10^{17} \text{cm}^{-3}$ .

#### IV. CONCLUSIONS

From the experimental fuse devised, we are able to conduct reproducible tests in order to evaluate the two physical parameters temperature and electron density. The first stage of the work consisted in the determination of the atomic species (together with their spectral parameters) that are present in the plasma. The following stage was to select those spectral lines we could use to evaluate the physical parameters.

The influence of the pressure broadening has to be quantified shortly for two reasons : first, it causes discrepancies in the determination of the temperature ; second, it would provide another way to evaluate the electron density.

#### ACKNOWLEDGEMENTS

We thank, both for their financial support and for their help for many discussions : Mr Barrault M R of Schneider Electric, Mr Rambaud M R of Ferraz SA, Mr V rit  J C of Electricit  de France, Mr Melquiond S and Mr Dides R of ALSTOM.

#### REFERENCES

- [1] Bezborodko P, Fauconneau J 1997 *Proc. Of XXIII Int. Conf. on Phenom. in Ion. Gas.* IV 69-9, Toulouse, July 17-22, 1997
- [2] Bussiere W, Bezborodko P, *Measurements of the time-resolved spectra of fuse arcs using a new experimental arrangement*, to be published in *J. Phys. D : Appl. Phys. (UK)*, Ref Number D/100661/PAP.(1999)
- [3] Massachusetts Institute of Technology 1969 *Wavelength Tables with Intensities in Arcs, Spark, or Discharge Tube* (Massachusetts M.I.T. Press)
- [4] Striganov A R, Sventitskii N S 1968 *Tables of Spectral Lines of Neutral and Ionised Atoms* (New York Washington IFI/Plenum)
- [5] Zaidel A N, Prokof'ev V K, Raiskii S M, Slavnyi V A, and Schreider E Y 1970 *Tables of Spectral Lines* (New York London IFI/Plenum)
- [6] NIST 1995 *Database for Atomic Spectroscopy version 1.0* (Gaithersburg National Institute of Standards and Technology)
- [7] Griem H R 1974 *Spectral Line Broadening by Plasmas* (New York and London : Academic Press)
- [8] Chikata T, Ueda Y, Murai Y, Miyamoto T, *Spectroscopic observations of arcs in current limiting fuse through sand* (ICEFA n 1 Liverpool April 1976 Proc. pp 114-121)

The first part of the document discusses the importance of maintaining accurate records of all transactions. It emphasizes that every entry should be clearly documented and verified. The text continues to describe various methods for ensuring the integrity of the data, including regular audits and cross-checking of entries. It also mentions the need for transparency and accountability in all financial dealings.

In the second section, the author details the specific procedures for handling incoming payments and outgoing expenses. It outlines the steps for recording each transaction, from the initial receipt to the final posting in the ledger. The text highlights the importance of timely recording and the use of standardized formats to facilitate easy review and analysis.

The third part of the document focuses on the reconciliation process, which is crucial for identifying and correcting any discrepancies. It provides a step-by-step guide for comparing the internal records with external statements, such as bank statements or supplier invoices. The author stresses that reconciliation should be performed regularly to prevent errors from accumulating.

Finally, the document concludes with a summary of the key principles of sound financial management. It reiterates the importance of accuracy, transparency, and regular review. The author encourages the reader to adopt these practices to ensure the long-term success and stability of their organization.

The second part of the document discusses the importance of maintaining accurate records of all transactions. It emphasizes that every entry should be clearly documented and verified. The text continues to describe various methods for ensuring the integrity of the data, including regular audits and cross-checking of entries. It also mentions the need for transparency and accountability in all financial dealings.



The third part of the document focuses on the reconciliation process, which is crucial for identifying and correcting any discrepancies. It provides a step-by-step guide for comparing the internal records with external statements, such as bank statements or supplier invoices. The author stresses that reconciliation should be performed regularly to prevent errors from accumulating.

Finally, the document concludes with a summary of the key principles of sound financial management. It reiterates the importance of accuracy, transparency, and regular review. The author encourages the reader to adopt these practices to ensure the long-term success and stability of their organization.